

Fusion of fractional vortex pairs and their transition to integer vortex controlled by optical power

Chunzhi Sun(孙春志), Xiangwei Chen(陈向炜), Huizhong Xu, and Guo Liang(梁果)
Citation: Chin. Phys. B, 2025, 34 (**5**): 054202. DOI: 10.1088/1674-1056/adb8b9
http://cpb.iphy.ac.cn; http://iopscience.iop.org/cpb

What follows is a list of articles you may be interested in

Broadband polarization-independent terahertz multifunctional liquid crystal coding metasurface based on topological optimization

Yu Chen(陈羽), Wu-Hao Cao(曹昊昊), Jia-Qi Li(李嘉琦), Ming-Zhe Zhang(张明哲), Xin-Yi Du(杜欣怡), Ding-Shan Gao(郜定山), and Pei-Li Li(李培丽)
Chin. Phys. B, 2025, 34 (**4**): 044205. DOI: 10.1088/1674-1056/adad55

Diffraction deep neural network-based classification for vector vortex beams

Yixiang Peng(彭怡翔), Bing Chen(陈兵), Le Wang(王乐), and Shengmei Zhao(赵生妹)
Chin. Phys. B, 2024, 33 (**3**): 034205. DOI: 10.1088/1674-1056/ad0142

Ultraviolet metalens and metalens array of focused vortex beams

Jinping Zhang(张金平), Yan Wang(王焱), Huan Yuan(袁欢), Zehao Wang(王泽豪), Yang Deng(邓阳),Chengzhi Huang(黄承志), Jiagui Wu(吴加贵), and Junbo Yang(杨俊波)
Chin. Phys. B, 2023, 32 (**6**): 064206. DOI: 10.1088/1674-1056/ac9d87

Generation of elliptical airy vortex beams based on all-dielectric metasurface

Xiao-Ju Xue(薛晓菊), Bi-Jun Xu(徐弼军), Bai-Rui Wu(吴白瑞), Xiao-Gang Wang(汪小刚), Xin-Ning Yu(俞昕宁), Lu Lin(林露), and Hong-Qiang Li(李宏强)
Chin. Phys. B, 2023, 32 (**2**): 024215. DOI: 10.1088/1674-1056/ac7cd0

Asymmetrical spiral spectra and orbital angular momentum density of non-uniformly polarized vortex beams in uniaxial crystals

Ling-Yun Shu(舒凌云), Ke Cheng(程科), Sai Liao(廖赛), Meng-Ting Liang(梁梦婷), and Ceng-Hao Yang(杨嶒浩)
Chin. Phys. B, 2023, 32 (**2**): 024211. DOI: 10.1088/1674-1056/ac7860

Fusion of fractional vortex pairs and their transition to integer vortex controlled by optical power

Chunzhi Sun(孙春志)[1], Xiangwei Chen(陈向炜)[1,†], Huizhong Xu[2], and Guo Liang(梁果)[1,‡]

[1] *Henan International Joint Laboratory of Optical Information Transmission and Application, Shangqiu Normal University, Shangqiu* 476000, *China*
[2] *Department of Physics and Astronomy, San Francisco State University, San Francisco, CA* 94132, *USA*

(Received 23 November 2024; revised manuscript received 19 January 2025; accepted manuscript online 21 February 2025)

The evolution of fractional vortex pairs in free space and nonlocal nonlinear media is studied. In free space, the off-axis fractional vortex pairs of the-same-sign topological charge (TC) will be merged to one integer vortex at the beam center, which is drastically different from the dynamics of integer vortex pairs. In nonlocal nonlinear media, the conversion between the fractional vortex pair and the conventional integer vortex can be readily achieved by only tuning the input optical power. Therefore our approach provides a convenient way to control the number of vortices and thus the number of optical tweezers by adjusting the input optical power. These results may find potential applications in optical manipulation of particles.

Keywords: vortex beams, orbital angular momentum, optical manipulation

PACS: 42.25.–p, 42.60.Jf

DOI: 10.1088/1674-1056/adb8b9 **CSTR:** 32038.14.CPB.adb8b9

1. Introduction

The orbital angular momentum (OAM), as a fundamentally new optical degree of freedom for photons, facilitates applications in a variety of fields including optical communication,[1] particle manipulation,[2,3] optical imaging and detection,[4–7] quantum information processing,[8–10] astronomy,[11,12] medical diagnosis,[13] and many more.[14] The simplest class of optical beam carrying the OAM is an optical vortex pointed out by Allen in 1992,[15] which can be quantitatively described by the helical phase structure $\exp(\mathrm{i}l\theta)$, where θ is the azimuth angle and l represents the topological charge (TC). Optical vortices with he helical phase $\exp(\mathrm{i}l\theta)$ in the forms of Laguerre–Gaussian beams,[15] high-order Bessel[16] and Mathieu[17] beams, are all the topological solutions of the paraxial Helmholtz equation, and can stably propagate in free space. As a result, multiple vortices of the same topological charge embedded in host beams will retain their relative positions in their linear propagation.[18,19] However, if vortices carry the opposite charges, they can attract each other and lead to their annihilation.[18,19] For more details on the properties of vortex beams with integer TC, the readers can refer to the classical review papers.[2,14,20]

In general, the value of TC, l, is commonly limited to integer numbers where the helical phase has a step of $2l\pi$. However, the values of the TC can also be non-integral, resulting in fractional vortex beams whose phase step is not an integer multiple of 2π.[21–23] Fractional vortex beams have special optical properties that differ significantly from those of integer vortex beams.[24] One of the key difference is that the fractional vortex beam cannot propagate stably in free space, instead exhibits a rich evolutionary process inducing complex amplitude and phase structures.[25–29] As a result of these unique properties not found in their integer counterparts, fractional vortex beams thus possess various promising potential applications. For instance, fractional vortex beams can expand the capacity in optical communication systems,[30] realize high-resolution imaging in radar imaging systems,[31] and achieve spatial entanglement in an infinite-dimensional subspace in quantum optics.[32]

In this work, we investigate the evolution of off-axis fractional vortex pairs of the same sign but different charges in both free space and nonlocal nonlinear media, and reveal the counterintuitive dynamics for the fractional vortex pairs. Unlike the conventional integer vortex pairs retaining their relative positions during propagation in free space, the off-axis fractional vortex pairs attract each other, and eventually merge to one integer vortex at the beam center. In nonlocally nonlinear media, the fusion of fractional vortex pairs as well as the transition between the fractional vortex pairs and unity integer vortex can be readily realized by adjusting the input optical power.

2. Fusion of fractional vortex pairs in free space

Consider a pair of fractional vortices of different charges

$$\varphi = A(x-q+\mathrm{i}y)^a(x+q+\mathrm{i}y)^b \exp\left(-\frac{x^2+y^2}{2w^2}\right), \quad (1)$$

†Corresponding author. E-mail: chenxiangwei@sqnu.edu.cn
‡Corresponding author. E-mail: liangguo0916@163.com

© 2025 Chinese Physical Society and IOP Publishing Ltd. All rights, including for text and data mining, AI training, and similar technologies, are reserved.

which are symmetrically embedded in a Gaussian host beam of width w. A is the pattern amplitude, a and b are the TCs of the two fractional vortices located at $(q,0)$ and $(-q,0)$ respectively. In the following discussions, we mainly focus on the case of $a+b=1$. In the paper, all the discussions are in the dimensionless coordinate system, and the dimensionless coordinates (x,y,z) are related to the physical coordinates (X,Y,Z) by the following coordinate transformation $x=X/w_0$, $y=Y/w_0$, $z=Z/Z_{\mathrm{R}}$, where w_0 is the beam width ($\sim$ μm) and $Z_{\mathrm{R}}=(2\pi/\lambda)w_0^2$ is the Rayleigh distance of the beam with wavelength λ.

In free space, the evolution of a paraxial optical beam is modeled by the dimensionless paraxial wave equation[33]

$$\mathrm{i}\frac{\partial\varphi}{\partial z}+\frac{1}{2}\left(\frac{\partial^2\varphi}{\partial x^2}+\frac{\partial^2\varphi}{\partial y^2}\right)=0, \tag{2}$$

where z is the longitudinal coordinate denoting the propagation direction of the beams, x and y are the transverse coordinates normal to z. The solution to the paraxial wave equation (2) can be expressed by the Fresnel diffraction integral[33]

$$\varphi(x,y,z)=-\mathrm{i}\frac{\exp(\mathrm{i}z)}{2\pi z}\int_{-\infty}^{\infty}\int_{-\infty}^{\infty}\varphi(x',y',0)\times\exp\left[\mathrm{i}\frac{(x-x')^2+(y-y')^2}{2z}\right]\mathrm{d}x'\mathrm{d}y', \tag{3}$$

where $\varphi(x,y,0)$ is the input beam at $z=0$, and takes the form of Eq. (1) in this paper. In fact, the fractional vortex is not an eigenmode to the paraxial wave equation, and can not maintain their amplitude distribution upon propagation. This is the main reason behind the evolution dynamics of the fractional vortex pairs.

Figure 1 shows the evolution of fractional vortex pairs carrying the same TCs $a=b=0.5$, where a very dynamical behavior is observed. Firstly, two off-axis fractional vortices merge into one vortex at the beam center as shown by both the intensity and phase distributions. Secondly, the beam loses its circular symmetry and evolves into an elliptic hollow beam during propagation, accompanied by beam rotation. Thirdly, a new pair of vortices of opposite charges (vortex dipole) emerges in the faint light intensity background. In order to make the newborn vortex dipole visible, we have plotted the intensity distribution using $\sqrt[4]{|\varphi|}$ instead of $|\varphi|^2$ in Figs. 1(a1)–1(c1). the newborn vortex dipole retains their relative positions and keeps rotating during propagation.

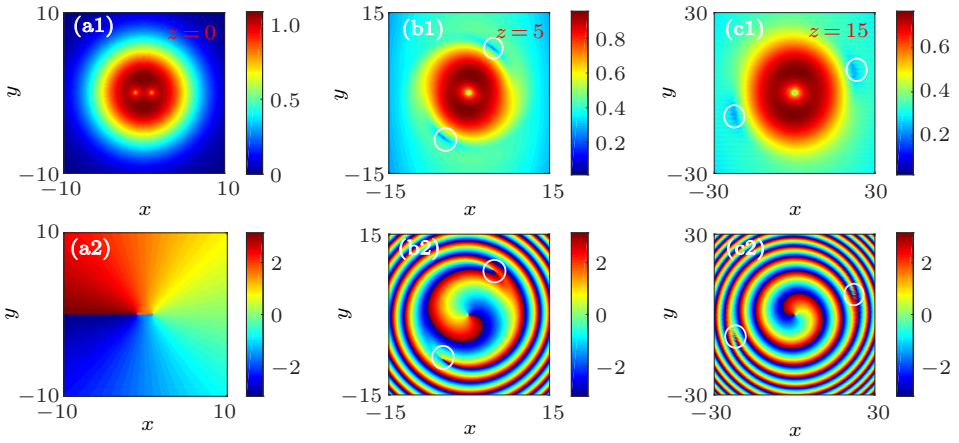


Fig. 1. Evolution of fractional vortex pair of Eq. (1) with $q=1$, $a=b=0.5$, and $w=2$. The top and bottom rows represent the light intensity and phase distribution respectively. In order to clearly show the newborn vortex dipole (symmetrically located at positions marked by white circles), $\sqrt[4]{|\varphi|}$ is plotted here instead of the actual intensity distribution.

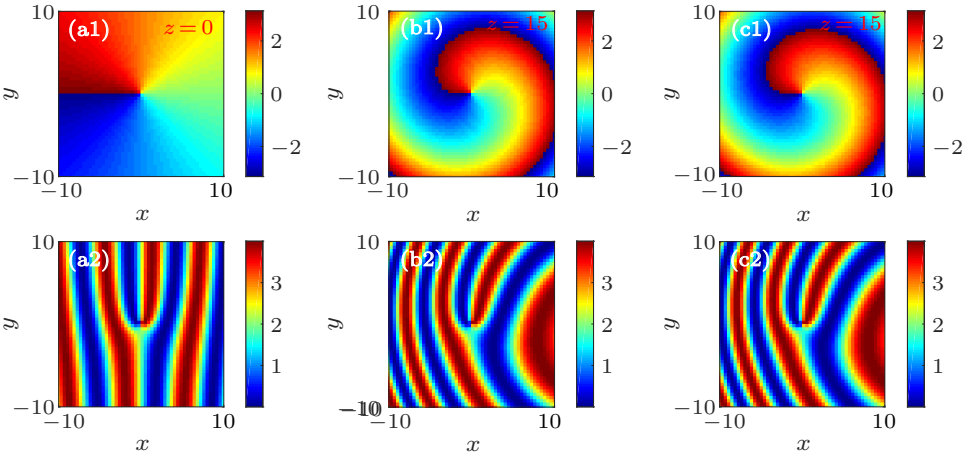


Fig. 2. Phase of a vortex beam with unit TC at $z=0$ (a1) and $z=15$ (b1); phase of the fractional vortex pair at $z=15$ (c1) under the same parameters as those in Fig. 1. Panels (a2)–(c2) show the interference patterns between the corresponding phase in panels (a1)–(c1) and a plane wave $\exp(\mathrm{i}x)$.

In order to investigate the TC value of the fused vortex by two off-axis fractional vortices, we compare the phase structure of the fused vortex with that of the traditional integer vortex at the same propagation distance in Fig. 2. As shown in Fig. 2(c1), the two off-axis phase singularities of fractional vortex pair evolve (fused) into the helical phase structure $\exp[\mathrm{i}\arctan(y/x)]$, which resembles that for a vortex beam with unit TC [see Fig. 2(b1)]. The interference patterns of the two phases with a plane wave are plotted in Figs. 2(b2)–2(c2), where the same fork-like structure is observed. When the phase of the fused vortex is combined with that of an integer vortex of TC equal to -1, the expected plane phase is indeed obtained, as shown in Fig. 3. Therefore, the off-axis fractional vortex pair of TC 0.5 are fused into an integer vortex of TC 1 at the center.

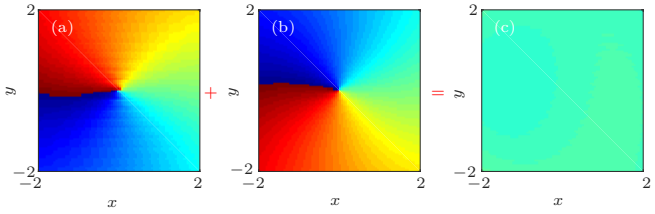


Fig. 3. Phase of fractional vortex pair (a), integer vortex of TC equal to -1 (b) at $z = 15$, and their combined phase (c).

Figure 4 shows the evolution of fractional vortex pairs with different off-axis distances q. The fusion of fractional vortex pairs can always occur regardless of the value of q. However, the intensity structure depends closely on q, the circularly symmetrical doughnut structure for small values of q exhibited by the Laguerre–Gaussian mode turns into Hermite–Gaussian-like modes for large q.

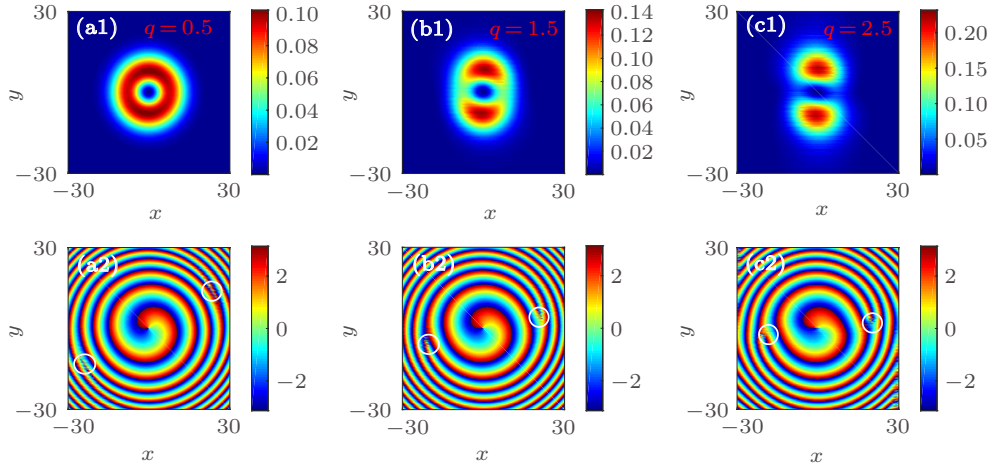


Fig. 4. Intensity $|\varphi|^2$ and phase structure at $z = 15$ of fractional vortex pair with different off-axis distances q. The white circles mark the positions of born vortex dipoles. The other parameters are the same as those in Fig. 1.

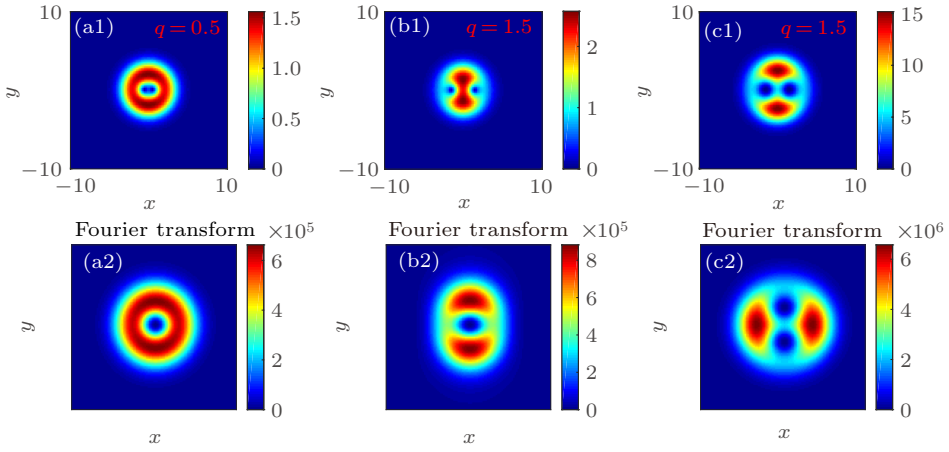


Fig. 5. Intensity $|\varphi|^2$ of fractional vortex pairs (a1)–(b1) and an integer vortex pair (c1) with off-axis distances q marked on top of every panel. Panels (a2)–(c2) show the corresponding Fourier transforms of panels (a1)–(c1). The parameters are taken as $a = b = 0.5$ for the fractional vortex pairs, while $a = b = 1$ for the integer vortex pair.

It can be seen from the above results that the fusion of fractional vortex pairs occur in fact in the far-field zone, where we can take an approximation $[(x-x')^2+(y-y')^2]/2z \approx \left[(x^2+y^2)-2xx'-2yy'\right]/2z$ and ignore the term $(x'^2+y'^2)/2z$ as long as $z \gg w^2/2$. Then equation (3) can be reduced to

$$\varphi(x,y,z) = -\mathrm{i}\frac{\exp(\mathrm{i}z)}{2\pi z}\exp\left(\mathrm{i}\frac{x^2+y^2}{2z}\right)\tilde{\varphi}\left(\frac{x}{z},\frac{y}{z}\right), \qquad (4)$$

where $\tilde{\varphi} = \int_{-\infty}^{\infty}\int_{-\infty}^{\infty}\varphi(x',y')\exp[-\mathrm{i}(xx'+yy')/z]\,\mathrm{d}x'\mathrm{d}y'$ can be regarded as the Fourier transform of the input beam $\varphi(x,y)$,

while $(x/z, y/z)$ is the equivalent transverse spatial frequency (k_x, k_y). In this sense, the far-field distribution of an input beam can be expressed by its Fourier transform, which can be confirmed by Fig. 5. The Fourier transform of a fractional vortex pair is an integer vortex nested at the beam center, which agrees with the aforementioned phenomenon that the off-axis fractional vortex pair of TC 0.5 is fused into an integer vortex of TC 1 at the beam center. For comparisons, we also give the Fourier transform of an integer vortex pair in Fig. 5, and reveal that two integer vortices indeed retain their relative positions. No TC fusion can occur for integer vortex pairs. In fact, the long work distance is not required in oder to observe the fusion of a fractional vortex pair in experiments as a lens system is ideal to perform a spatial Fourier transform on a given optical amplitude distribution.[33] If the fractional vortex pair is produced in the front focal plane of a lens, its Fourier transform (the fused integer vortex) will appear in the rear focal plane of the lens.

We also discuss the evolution of fractional vortex pairs with different TCs as shown in Fig. 6. Because the TCs of the fractional vortex pair $a+b=1$, they all can be fused into an integer vortex of TC 1 at the beam center in the far-field zone. Besides, the vortex dipoles can be created in the faint light intensity background for all cases. As the ratio of TCs for the two fractional vortex components, a/b, changes, both the intensity pattern and its orientation behave differently while the phase distribution stays the same as expected.

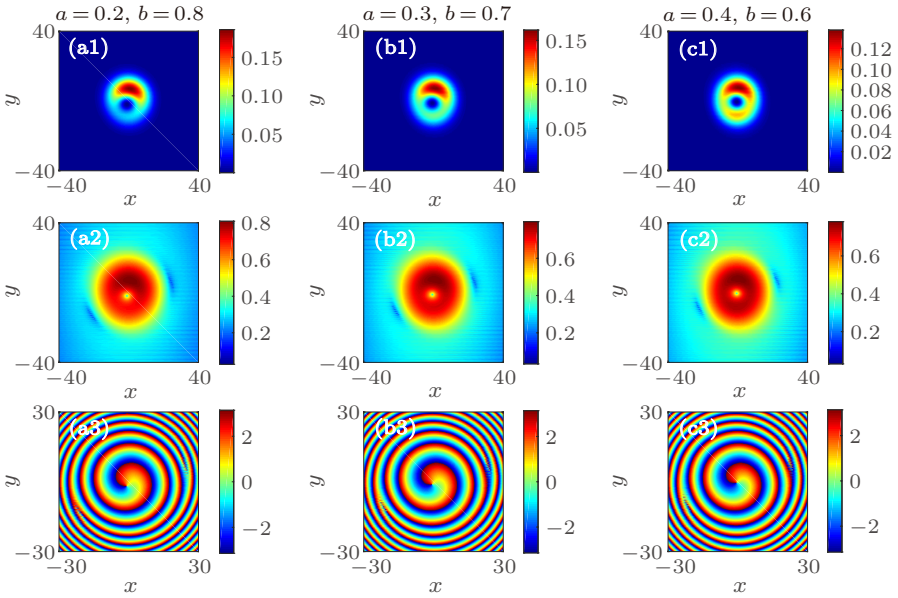


Fig. 6. Intensity $|\varphi|^2$ (the first row), $\sqrt[4]{|\varphi|}$ (the second row), and phase (the third row) of fractional vortex pair at $z=15$. The parameters of (a,b) are taken as (0.2,0.8) (the first column), (0.3,0.7) (the second column), and (0.4,0.6) (the third column).

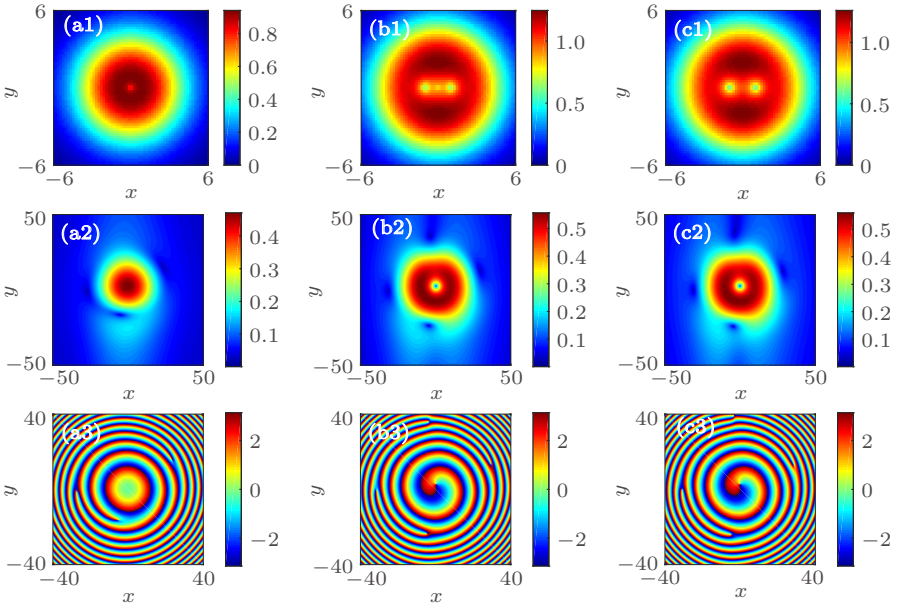


Fig. 7. Intensity distribution of fractional vortex beams at $z=0$ (the first row), and their intensity (the second row), and phase (the third row) distribution at $z=20$. The optical pattern is assumed to $A(x-q+\mathrm{i}y)^a(x+q+\mathrm{i}y)^b(x+\mathrm{i}y)^c\exp\left[-(x^2+y^2)/(2w^2)\right]$. The parameters of (a,b,c) are taken as (0,0,0.3) (the first column), (0.5,0.5,0.2) (the second column), and (0.6,0.6,0) (the third column). The intensity is represented by $\sqrt[4]{|\varphi|}$, and the off-axis distance $q=1$.

Now we extend our consideration to the case of $a+b>1$. Figure 7 shows the evolution of a fractional vortex pair of Eq. (1) with $a=b=0.6$. From an evolutionary perspective, it is equivalent to the combination of one off-axis fractional vortex pair with TC $a=b=0.5$ and a third on-axis fractional vortex with TC $c=0.2$ as shown in Fig. 7. The off-axis fractional vortex pair with TC $a=b=0.6$ will merge into an integer vortex of unity TC at the center, which is same as the case discussed above. However, there are four new vortices appearing in the faint light intensity background. Among the newborn vortices, three of them come from the fractional vortex with TC $c=0.2$ (that in fact amounts to $0.6\cdot 2-1$).

3. Conversion between fractional vortex pair and conventional integer vortex in nonlocal nonlinear media

As discussed above, fractional vortex beams are not the eigenmodes to the paraxial wave equation (2) thus cannot have stable propagation in free space. However, the properties of nonlocal nonlinear media have been proven to stabilize beams carrying the fractional OAM such as the fractional Laguerre–Gaussian patterns.[34] Furthermore, the beam diffraction can be balanced by the self-focusing effect in nonlinear media, and form solitons or breathers which can propagate over long distances.[35] In the strongly nonlocal nonlinear media, where the response length of media is much larger than the beam width, the evolution of spatial optical beams can be described by the Snyder–Mitchell model[35] $\mathrm{i}\partial_z\varphi+(1/2)(\partial_x^2\varphi+\partial_y^2\varphi)-(1/2)P_0\gamma^2(x^2+y^2)\varphi=0$, where γ is a material constant, and $P_0=\iint|\varphi(x,y)|^2\mathrm{d}x\mathrm{d}y$ is the input optical power. It should be noted that for the Snyder–Mitchell model the optical power is a conservative quantity. The Snyder–Mitchell model formally resembles the Schrödinger equation with an external harmonic potential,[36] where γ plays the role of the modulation depth of the external potential. The evolution of beams in the Snyder–Mitchell model is equivalent to their two-dimensional fractional Fourier transform[37,38]

$$\varphi(x,y,z)=\hat{F}_\alpha\{\varphi(x,y,0)\}\exp(-\mathrm{i}\alpha), \tag{5}$$

with the fractional Fourier transform operator reading

$$\begin{aligned}&\hat{F}_\alpha\{f(x,y,0)\}\\&=\frac{\exp[\mathrm{i}(\alpha-\pi/2)]}{2\pi\sin\alpha}\exp\left[\frac{\mathrm{i}(x^2+y^2)}{2\tan\alpha}\right]\\&\times\iint\exp\left[\frac{\mathrm{i}(x'^2+y'^2)}{2\tan\alpha}-\frac{\mathrm{i}(x'x+y'y)}{\sin\alpha}\right]f(x',y',0)\mathrm{d}x'\mathrm{d}y',\end{aligned}$$

where $\alpha=\sqrt{P_0}\gamma z$ is the order of the fractional Fourier transform. In the special case that $\alpha=\pi/2$, the fractional Fourier transform (5) will be deduced to the standard Fourier transform.

From Eq. (5), we can predict that an optical beam would experience a periodic evolution with the period $\Delta z=2\pi/\sqrt{P_0}\gamma$ (derived from the equation $\alpha=2\pi$). While, for an axis-symmetric distribution, the optical field can restore to its initial shape after the half period $\Delta z/2$. Since the response length of a nonlinear medium cannot be changed once the material is manufactured, it will be impractical to tune the value of alpha by changing γ in experiments. Instead, we can choose to control α by only adjusting the input optical power P_0. Figure 8 displays an example of conversion between fractional vortex pair and their fused vortex controlled by the input optical power at the fixed propagation distance $z=\pi$. In the field of optical manipulation, vortex beams can function like optical tweezers to trap and manipulate particles.[2,3] Therefore, we can provide a convenient way to control the number of vortices and thus the number of optical tweezers by tuning the input optical power.

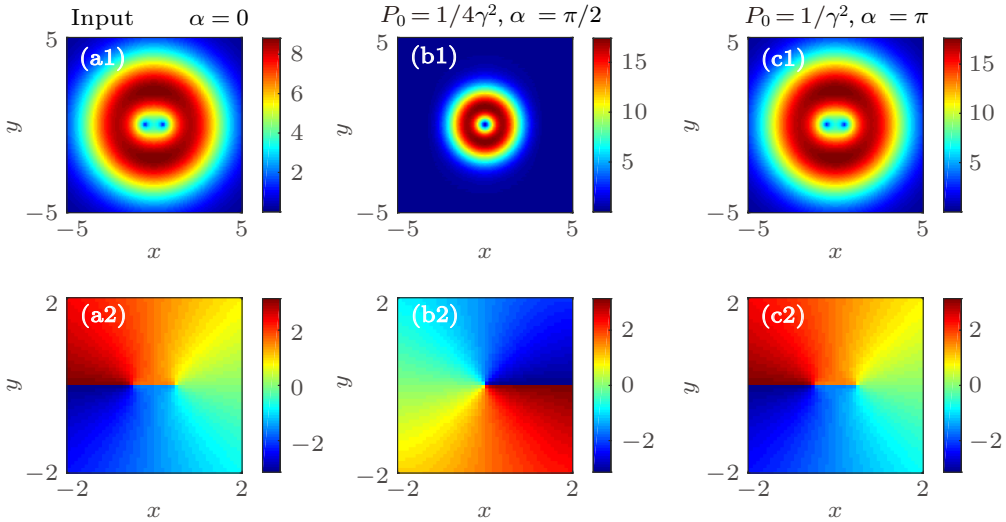


Fig. 8. Optical power controllable conversion between fractional vortex pair and their fused vortex. The first and second column represent the amplitude $|\varphi|$ and phase. The parameters are taken as $q=0.5$, $a=b=0.5$, $w=2$, and $z=\pi$.

4. Conclusion

The dynamics of off-axis fractional vortex pairs is discussed in both free space and nonlocal nonlinear media. In free space, unlike the conventional integer vortex pairs which can retain their relative positions during propagation, an off-axis fractional vortex pair will merge into an integer vortex at the beam center. During the fusion, new vortices can be created in the faint light intensity background accompanied by energy rotating. In nonlocal nonlinear media, at a given propagation distance the transition between the fractional vortex pair and the merged unity integer vortex can be readily realized by only changing the input optical power. This type of optical-power-controllable conversion can also be realized in other physical configurations such as gradient refractive index media and nonlinear media with an external potential.

Acknowledgements

Project supported by the International Scientific and Technological Cooperation Projects of Henan Province, China (Grant No. 242102520010), the Natural Science Foundation of Henan Province, China (Grant No. 252300421307), and the Training Program for Young Backbone Teachers of Higher Education Institutions in Henan Province, China (Grant No. 2023GGJS130).

References

[1] Wang J, Yang, J Y, Fazal I M, Ahmed N, Yan Y, Huang H, Ren Y X, Yue Y, Dolinar S and Tur M 2012 *Nat. Photon.* **6** 488
[2] Padgett M and Bowman R 2011 *Nat. Photon.* **5** 343
[3] Yang Y J, Ren Y X, Chen M Z, Arita Y and Rosales-Guzmán C 2021 *Adv. Photon.* **3** 034001
[4] Tamburini F, Anzolin G, Umbriaco G, Bianchini A and Barbieri C 2006 *Phys. Rev. Lett.* **97** 163903
[5] Qiu X D, Li F S, Zhang W H, Zhu Z H and Chen L X 2018 *Optica* **5** 208
[6] Courtial J, Robertson D A, Dholakia K, Allen L and Padgett M J 1998 *Phys. Rev. Lett.* **81** 4828
[7] Lavery M P J, Speirits F C, Barnett S M and Padgett M J 2013 *Science* **341** 537
[8] Nicolas A, Veissier L, Giner L, Giacobino E, Maxein D and Laurat J 2014 *Nat. Photon.* **8** 234
[9] Ding D S, Zhang W and Zhou Z Y, *et al.* 2015 *Phys. Rev. Lett.* **114** 50502
[10] Otte E, Rosales-Guzmán C, Ndagano B, Denz C and Forbes A 2018 *Light Sci. Appl.* **7** 18009
[11] Lee J H, Foo G, Johnson E G and Swartzlander G A 2006 *Phys. Rev. Lett.* **97** 53901
[12] Tamburini F, Thidé B, Molina-Terriza G and Anzolin G 2011 *Nat. Phys.* **7** 195
[13] Gianani I, Suprano A, Giordani T, Spagnolo N, Sciarrino F, Gorpas D, Ntziachristos V, Pinker K, Biton N, Kupferman J and Arnon S 2020 *Adv. Photon.* **2** 036003
[14] Shen Y J, Wang X J, Xie Z W, Min C J, Fu X, Liu Q, Gong M L and Yuan X C 2019 *Light: Sci. Appl.* **8** 90
[15] Allen L, Beijersbergen M W, Spreeuw R J C and Woerdman J P 1992 *Phys. Rev. A* **45** 8185
[16] Garcés-Chávez V, McGloin D, Padgett M J, Dultz W, Schmitzer H and Dholakia K 2003 *Phys Rev. Lett.* **91** 093602
[17] López-Mariscal C, Gutiérrez-Vega J C, Milne G and Dholakia K 2006 *Opt. Express* **14** 4182
[18] Basistiy I, Bazhenov V, Soskin M S and Vasnetsov M V 1993 *Opt. Commun.* **103** 422
[19] Indebetouw G 1993 *J. Mod. Opt.* **40** 73
[20] Yao A M and Padgett M J 2011 *Adv. Opt. Photon.* **3** 161
[21] Beijersbergen M W, Coerwinkel R P C, Kristensen M and Woerdman J P 1994 *Opt. Commun.* **112** 321
[22] Basistiy I V, Soskin M S and Vasnetsov M V 1995 *Opt. Commun.* **119** 604
[23] Vasnetsov M, Basistiy I and Soskin M 1998 *Proc. SPIE* **3487** 29
[24] Zhang H, Zeng J, Lu X Y, Wang Z Y, Zhao C L and Cai Y J 2022 *Nanophotonics* **11** 241
[25] Berry M V 2004 *J. Opt. A: Pure Appl. Opt.* **6** 259
[26] Tao S H and Yuan X C 2004 *J. Opt. Soc. Am. A* **21** 1192
[27] Alperin S N and Siemens M E 2017 *Phys. Rev. Lett.* **119** 203902
[28] Yang Z S, Zhang X, Bai C L and Wang M H 2018 *J. Opt. Soc. Am. A* **35** 452
[29] Hu J T, Tai Y P, Zhu L H, Long Z X, Tang M M, Li H H, Li X Z and Cai Y J 2020 *Appl. Phys. Lett.* **116** 201107
[30] Zhu G X, Bai Z Y, Chen J Y, Huang C R, Wu L P, Fu C L and Wang Y P 2021 *Opt. Express* **29** 28452
[31] Liu H Y, Wang Y, Wang J, Liu K and Wang H Q 2021 *IEEE Antennas Wirel. Propag. Lett.* **20** 948
[32] Oemrawsingh S S R, Ma X, Voigt D, Aiello A, Eliel E R, Hooft G W 't and Woerdman J P 2005 *Phys. Rev. Lett.* **95** 240501
[33] Haus H A 1984 *Waves and Fields in Optoelectronics* (Prentice-Hall, Englewood Cliffs, NJ)
[34] Pan X J, Zhang C F, Deng C J, Li Z L and Wang Q 2021 *Res. Phys.* **27** 104511
[35] Snyder A W and Mitchell D J 1997 *Science* **276** 1538
[36] Zhong W P and Belić M R 2010 *Phys. Rev. E* **81** 056604
[37] Lu D Q, Hu W, Zheng Y J, Liang Y B, Cao L G, Lan S and Guo Q 2008 *Phys. Rev. A* **78** 043815
[38] Liang G, Chen X W and Xu H Z 2024 *Opt. Lett.* **49** 4871